Asian Journal of Chemistry Vol. 21, No. 5 (2009), 3885-3891

Effect of EDTA (Acid and Salt) on The Formation of Hydroxyapatite by Sol Gel Processing: A Comparative Study

H. KHIREDDINE*, S. SAOUDI, S. ZIANI, S. MESKI and S. MESKOUR†
Laboratory of Environnement Engineering, Faculty of Technology
University of Béjaia, 06 000 Béjaia, Algéria
E-mail: khiredine.hafit@gmail.com

Hydroxyapatite (HAP), $Ca_{10}(PO_4)_6(OH)_2$, is a bioceramic which have application in bone substituate materials. It is similar to the mineral phase of human bone. The preparation of hydroxyapatite powders or films with controlled morphology, stoichiometry, crystallinity and particular size in the nanometer range has the main role in production of materials. It depends on the precursors, solvent and temperature. Chelating agents (ethylenediamine tetra-acetic acid, EDTA, acid and sodium salt) have been used to prepare inorganic powders by sol gel process. We have investigated the effect of nature EDTA (acid or sodium) on the composition, structure and morphology of hydroxyapatite nanocrystals. It is found that EDTA plays an important role in synthesis of final HAP nanostructures. The samples were studied by X-ray powder diffraction analysis (XRD), infrared spectroscopy (IR) and scanning electron microscopy (SEM). The results showed that the carbonate substitution occurred in the phosphate sites increased in the case of HAP-EDTA sodium, which is expected to improve the bioactivity, the solubility and the osteointegration.

Key Words: Hydroxyapatite, Sol gel, EDTA.

INTRODUCTION

Bioceramics are special compositions of ceramic materials in the form of powders, coatings or bulk devices that are used to repair, augment or replace diseased or damaged tissues, usually bones, joints or teeth[1,2].

The damaged tissue can be replaced by endogenous tissues, but such replacement may lead to several problems. The use of endogenous bone substance involves additional surgery. Moreover, endogenous bone is available only in limited quantities. The disadvantages of exogenous bone implants are that they may be rejected by the human body, diseases may be transmitted together with the implant and also the clinical performance of exogenous bone is considerably inferior to fresh endogenous graft material. For these reasons, there is a growing need for fabrication of artificial bone implants.

†Laboratoire de Traitement et Mise en Forme des Polymères, University of Boumerdes, 35000 Boumerdes, Algeria.

The bioactive calcium phosphates, for example, hydroxyapatite, tricalcium phosphate and amorphous calcium phosphate, have been studied as hard tissue implant materials because it is similar to the natural mineral apatite found in bone[3-5] and when implanted has been shown to be a biocompatible substance that chemically bonds with bone. Furthermore, it has also been studied of other non medical applications such as packing media for column chromatography, catalysts[6,7], removal of heavy metals from contaminated soils and wastewater[8,9] or confinement of nuclear wastes[10], due to their stability and capacity to retain durability a large variety of trace elements.

The composition, physico-chemical properties, crystal size and morphology of synthetic apatite's are extremely sensitive to preparative conditions for diverse applications. A particular attention has been paid to the synthesis of hydroxyapatite, $Ca_{10}(PO_4)_6(OH)_2$, which is frequently used as reference materials in biomineralization and biomaterial studies. Hence researches have tried to customerize its properties such as bioactivity, mechanical strength, solubility, osteoconductive properties by controlling its composition, morphology and particle size[11-13].

Among the alternative methods, sol gel synthesis of HAP ceramics has recently attracted much attention, due to its many advantages which include high product purity, homogeneous composition and low synthesis temperature[4,14-16]. Chelating agents including EDTA have been tested to produce hexagonal HAP in hydrothermal condition[17], to synthesis of HAP by microwave irradiation[18]. Arce *et al.*[19] have suggested the preparation of HAP by decomposition of Ca-EDTA complex from aqueous solution of $CaCl_2 \cdot 2H_2O$. However, the use of nitrate or chloride of calcium as a precursor affect the structure of hydroxyapatite.

Among these bioactive materials, B-type carbonated hydroxyapatite sodium is the apatite which has the quite similarity with biological natural apatite[20].

The purpose of the present investigation was to compare the composition, morphology and structure of hydroxyapatite powder formed by 2 different EDTA complex, acid and salt, using sol gel methods where the precursor of Ca was calcium acetate, because CH_3COO^- ions are not incorporated in to the apatite[21].

EXPERIMENTAL

Powder synthesis: Powders were prepared by an aqueous sol gel process. Calcium acetate monohydrate ($Ca(CH_3COO)_2 \cdot H_2O$, reagent grade, Aldrich, France), was selected as Ca precursor. It was first dissolved in 0.1 M of CH_3COOH at 60 °C. To this solution an aqueous solution (60 °C) of diammonium hydrogenophosphate [$(NH_4)_2HPO_4$, reagent grade, Aldrich, France] precursor of P, was added. The solutions were mixed in Ca/P molar ratio of 1.67. The mixture was continuously stirred for *ca*. 2 h at 60 °C. In the following step, ethylene diamine tetraacetic acid or its sodium salt as complexing agents was added to the above solution, a white transparent gel was obtained. The slow evaporation was continued under stirring till the contents turned in to the homogenous paste. The material was first dried at 100 °C and then heated at 1000 °C for 2 h in a mufle furnace. The cakes were ground to fine powders for characterization studies.

Characterization: Dried powders were subjected to thermal analysis (DTA/TGA) with a heating of 25 to 700 °C in nitrogen atmosphere (flow rate 200 mL/min) using a Setaram TG-DTA 92, at heating rate of 10 °C/mn. Crystal structure identification of HAP-EDTA samples was performed using X-ray diffraction (phillips X'pert prof, analytical, systeme MPD), using Cuka radiation in the range $25 \leq 2\theta \leq 40$ at a scan speed of 4 °/min.

The presence of chemical groups of HAP-EDTA surface was investigated in the spectral region 4000-400 cm^{-1} using Fourier transformation infrared spectrophotometer (Shimadzu FTIR 8300). The KBr disc technique was employed using few mg of HAP-EDTA powder (sample/KBr = 1/200).

For the morphology characterization, well polished HAP samples were studied using scanning electron microscopy (SEM), philips XL 20 equiped for X ray microanalysis (EDAX), detector SUTW-saphire resolution: 129.42.

RESULTS AND DISCUSSION

The DTA-TGA curves recorded for HAP-EDTA acid and salt samples in the range of 25 and 700 °C, is represented in Fig. 1.

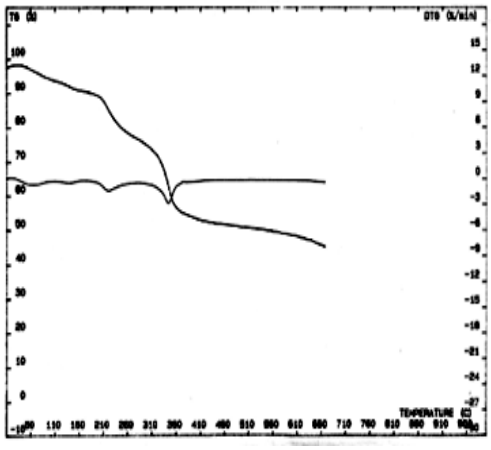

Fig. 1. DTA/TGA curves of HAP-EDTA

The TG curves of HAP-EDTA powders exhibit three weight loss stages which correspondent to three peaks endothermic at DTA curve. The first stage was observed from 60 to 180 °C, around 10 % weight loss. This can be attributed to desorption of water molecules adsorbed on the crystallite surface. The second stage of weight loss (20 %) on the TG curves was observed between 205 and 330 °C. This stage corresponds to the condensation of HPO_4^{2-} ions to $P_2O_7^{4-}$ according to the following reactions[22]:

$$2HPO_4^{2-} \rightarrow P_2O_7^{4-} + H_2O$$

and the removal of residual NH_4^+, CH_3COO^- and water strongly linked in structure apatite, probably due to intercrystalline water[22,23]. This weight loss is also confirmed by sharp peaks endothermic (220 °C) in the DTA plot. The third stage of weight loss (*ca*. 15 %) of the TG curves was observed between 330 and 350 °C and the large endothermic peak observed in DTA curves was around 350 °C. This weight loss in this region can be attributed to thermal dissociation of hydroxyl group and their reaction[24] with $P_2O_7^{4-}$:

$$P_2O_7^{4-} + 2OH^- \rightarrow 2PO_2^{3-} + H_2O$$

The crystallization peak's (*ca*. 750 °C[16,25]) was not observed because the range temperature study was 25 to 700 °C.

The FTIR spectrum of the final powders sintered at 1000 °C, shows the characteristic peaks of hydroxyapatite (Fig. 2). These bands corresponding to the phosphate, ν_3 PO_4^{3-} (1100-1030 cm^{-1}); ν_1 PO_4^{3-} (960-900 cm^{-1}); ν_4 PO_4^{3-} (600-550 cm^{-1}), ν_2 PO_4^{3-} (470 cm^{-1}), hydroxyl groups (OH), 3650 cm^{-1} (strong) and 650 cm^{-1} (small)[15]. Particulary the FTIR spectrum of HAP-EDTA sodium salt yet shows broad peaks, typical of amorphous products. The broadness of the XRD spectrum, Fig. 3, provides support for this tentative conclusion. with characteristic bands carbonate ν_3 CO_3^{2-} (1480, 1400 cm^{-1}) and ν_2 CO_3^{2-} (873 cm^{-1}). The band at 873 cm^{-1} can be attributed[26] to HPO_4^{2-}. The presence of ν_3 CO_3 group indicates that the HAP-EDTA sodium salt could be a B-type carbonated apatite, *i.e.*, CO_3-for-PO_4 substitutions. This substitutions leads to decrease of the a-axis of the apatite lattice and involve to the increase in Ca/P ratio, according to Slosarczyk *et al.*[27]. They obtained non-stoichiometric carbonated apatite. FTIR spectra of HAP-EDTA sodium salt shows ν_3 band of phosphate (PO_4^{3-}) appear as a single intense band (1020 cm^{-1}) and weak band at 1065 cm^{-1} whereas in HAP-EDTA acid it appears as three distinct bands at 1100, 1030 and 1000 cm^{-1}. The absence of -OH group at 650 cm^{-1} in HAP-EDTA acid may suggest as a result due to the character acid of a complex which involve positively charged apatite. In addition to the above peaks, the calcite ($CaCO_3$) absorption peak appeared

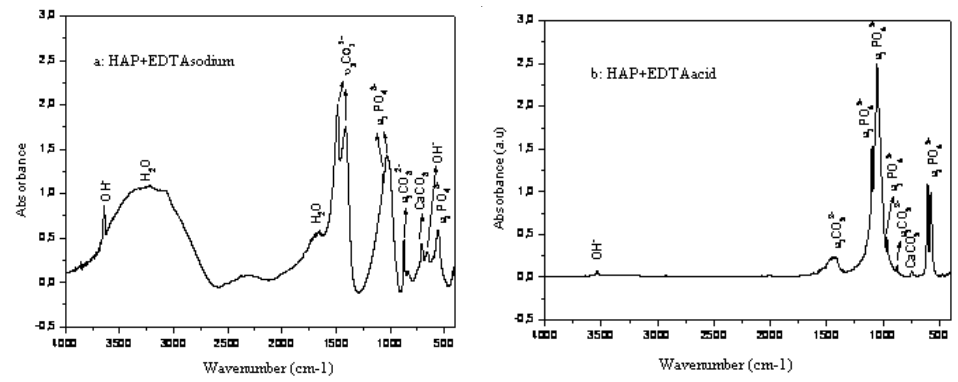

Fig. 2. FT-IR spectra of hydroxyapatite synthesized at 1000 ºC using EDTA

appeared around 720 cm^{-1}, in the two powders, which evident from the XRD pattern (Fig. 3). This was probably due to the stirring bad solution or impurity phase. The IR results obtained are completely consistent with the analyses carried out by XRD measurements.

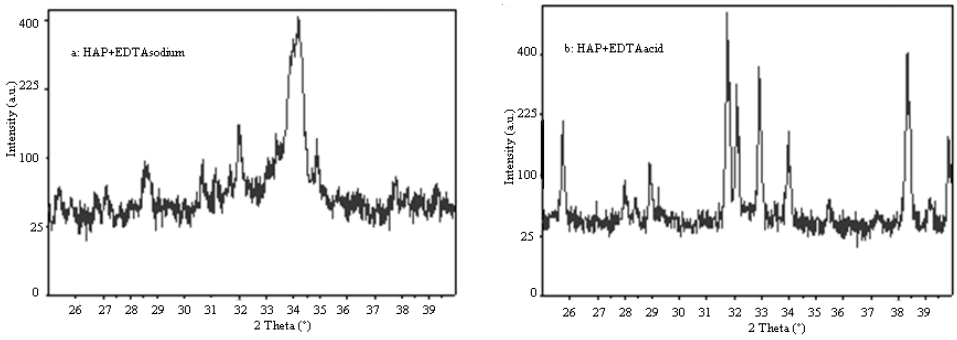

Fig. 3. XRD patterns of hydroxyapatite synthesized at 1000 ºC using EDTA

Fig. 3 shows the XRD pattern for the both powder's hydroxyapatite. In Fig. 3a three strong characteristic diffraction peaks for HAP-EDTA acid at 2θ = 31-34° [(211), (300) and (112)][28] were found. However the results shows a poor crystalline nature of apatite HAP-EDTA sodium, with broad diffracted peaks. Two broad peaks at about 30.5 and 31.2 were observed, together with considerable amount of amorphous phase. These two broad peaks appear to be tricalcium phosphate [$Ca_3(PO_4)_2$][29] and monetite ($CaHPO_4$)[19]. It is suggested that the relative intensity of peak (300) of HAP-EDTA sodium increase more than that of HAP-EDTA acid, which shows HAP-EDTA sodium particles may be oriented along c-axis[17]. It is also noticed that the crystallographic behaviour of HAP-EDTA sodium resembles to that XRD pattern of biological apatite[30]. Therefore it shows the formation of small amounts of $CaCO_3$ (2θ = 28.5 °) which corroborated with IR analysis.

SEM micrographs of the two powders were represented in Fig. 4. As seen in the figure, particles sizes of both samples are quiet different. All of the investigation powders consist of spherule agglomerates (particle distribution in the range 500 nm) which can be observed in the case HAP-EDTA acid and a mixed needle-shaped nano-particles which has a width of 3 μm and length of 20-40 μm and particle spherical (Ø ≤ 1 μm) for HAP-EDTA sodium. According to these results, it is estimated that the particles shown in SEM micrographs (Fig. 4a) consist of several crystallites[17,19].

The EDX analyses (Fig. 5) have shown the presence of sodium which is as abundant trace element as calcium and phosphorus in natural bone and tooth mineral. It has an important role in cell adhesion and also in the bone metabolism and resorption process. It has been reported that substitution of calcium by sodium creates supplementary vacancies in calcium sites, the model proposed by Vignole[31] was:

$$Ca_{10-x}\ Na_{2x/3}\ V_{x/3}(PO_4)_{6-x}\ (CO_3)_x\ (H_2O)_x\ (OH)_{2-x/3}\ V_{x/3} \text{ with } 0 \le x \le 3$$

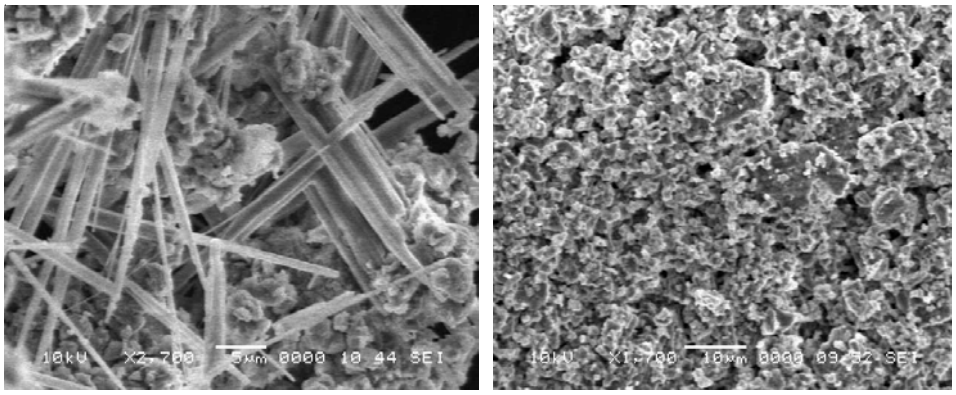

(a) HAP + EDTA sodium (b) HAP + EDTA acid

Fig. 4. SEM micrographs of hydroxyapatite synthesized at 1000 ºC using EDTA

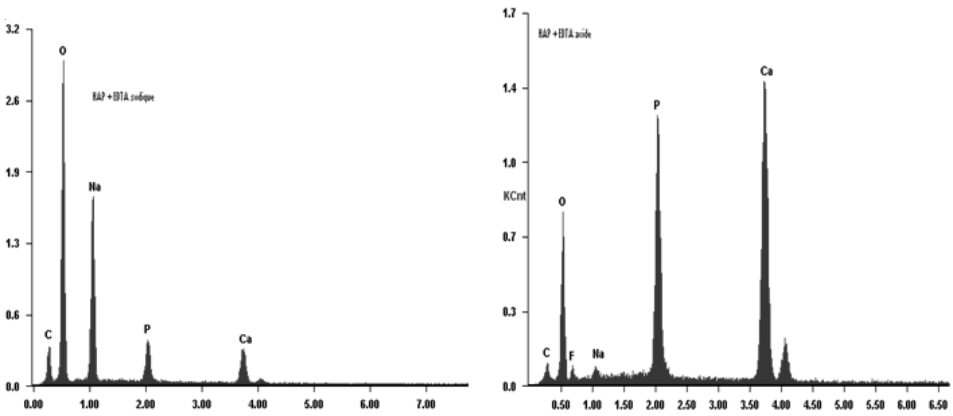

(a) HAP + EDTA sodium (b) HAP + EDTA acid

Fig. 5. EDAX of hydroxyapatite synthesized at 1000 ºC using EDTA

It could be proposed that the morphology depends of the character of EDTA. EDTA is a strong complex reagent with Ca^{2+}, which leads to the formation of Ca-EDTA complexes. In solution, the stability of EDTA sodium is higher than that of acid EDTA (pH↑). So the presence of OH^- ions on the facets control the growth rates in various crystal facets[18]. The presence of β-$Ca_3(PO_4)_2$, β-TCP is attractive, actually a biphasic calcium phosphate (BCP) composite has been developed by several authors[32-34].

Conclusion

The composition, crystalline degree and the morphology of the obtained powder are dependent on EDTA character. This study reveals the feasibility of producing hydroxyapatite powder with structural and chemical functionalities quite similar to biological apatite. The chemical composition of sodium HAP-EDTA was a B-type carbonate hydroxyapatite with small carbonate ions occupying hydroxyl sites leading to A-type carbonate apatite. The presence of sodium in this apatite is characterized by EDX analysis. The ideal formula is actually never identified. The precursors,

the method and some others parameters, regular the composition of powder hydroxyapatite. This, vary according to the possibilities of anionic and cationic substitutions and the existence of different types of in vacancies, several models have been proposed[26]. In present case, we estimated a small quantities of OH^- substituted by CO_3^{2-} (873 cm^{-1}), thus the following formula is proposed:

$$Ca_{10-x}\ Na_{2x/3}\ V_{x/3}(PO_4)_{6-x}\ (CO_3)_x\ (H_2O)_x\ (OH)_{2-x/3\ -2\varepsilon}\ V_{x/3}\ (CO_3)_\varepsilon$$

with $0 \le x \le 3$; V: vacancies.

REFERENCES

1. C. Chevallard and P. Guenoun, *Bull. de la S.F.P.*, **155**, 5 (2006).
2. A.C. Derrien, Ph.D. Thesis, University of Rennes, France (2004).
3. G. Montel, G. Bonel, J.C. Trombe, J.C. Heughebaert and C. Rey, *Pure Appl. Chem.*, **52**, 973 (1980).
4. D. Liu, Q. Yang, T. Troczynski and W.J. Tseng, *Biomaterials*, **23**, 1679 (2002).
5. T. Kokubo, H.M. Kim and M. Kawashita, *Biomaterials*, **24**, 2161 (2003).
6. K. Cheng, W. Weng, G. Han, P. Du, G. Shen, J. Yang and J.M.F. Ferreira, *Mater. Chem. Phys.*, **78**, 767 (2003).
7. W. Weng and J.L. Baptista, *J. Eur. Ceram. Soc.*, **17**, 1151 (1997).
8. J. Gómez, P. Sanchez, P.J. Morando and D.S. Cicerone, *Chemosphere*, **64**, 1015 (2006).
9. F. Fernane, M.O. Mecherri, P. Sharrock, M. Hadioui, H. Lounici and M. Fedoroff, *Mater. Charact*, **59**, 554 (2008).
10. F.G. Simon, V. Biermann and B. Peplinski, *Appl. Geochem.*, **23**, 2137 (2008).
11. R.M. Trommer, L.A. Santos and C.P. Bergmann, *Surface Coatings Technol.*, **201**, 9587 (2007).
12. N. Dumelie, H. Benhayoune, D. Richard, D. Laurent-Maquin and G. Balossier, *Mater. Charact.*, **59**, 129 (2008).
13. L. Gran and R. Pilliar, *Biomaterials*, **25**, 5303 (2004).
14. M.H. Fathi, A. Hanifi and V. Mortazavi, *J. Mater. Process. Technol.*, **202**, 536 (2008).
15. A.H. Rajabi-Zamani, A. Behnamghader and A. Kazemzadeh, *Mater. Sci. Eng.*, **28**, 1326 (2008).
16. I. Bogdanoviciene, A. Beganskiene, K. Tõnsuaadu, J. Glaser, H.-Jürgen Meyer and A. Kareiva, *Mater. Res. Bull.*, **41**, 1754 (2006).
17. R. Zhu, R. Yu, J. Yao, D. Wang and J. Ke, *J. Alloys Comp.*, **457**, 555 (2008).
18. J. Liu, K. Li, H. Wang, M. Zhu and H. Yan, *Chem. Phys. Lett.*, **396**, 429 (2004).
19. H. Arce, M.L. Montero, A. Saenz, V.M. Castano, *Polyhedron*, **23**, 1897 (2004).
20. Y. Doi and T. Shibutani, *J. Biomed. Mater. Res.*, **39**, 603 (1998).
21. F. Miyaji, Y. Kono and Y. Suyama, *Mater. Res. Bull.*, **40**, 209 (2005).
22. M. Banu, Ph.D. Thesis, INP de Toulouse, France (2005).
23. S. Kim and P.N. Kumta, *Mater. Sci. Eng. B*, **111**, 232 (2004).
24. L. Winand, Ph.D. Thesis, University of Liège, Belgium (1961).
25. H.K. Varma and S.S. Babu, *Ceram. Int.*, **31**, 109 (2005).
26. J.P. Lafon, Ph.D. Thesis, University of Limoge, France (2004).
27. A. Slosarczyk, Z. Paszkiewicz and C. Paluszkiewicz, *J. Mol. Struct.*, **704**, 333 (2004).
28. Powder Diffraction File #9-432, International Centre for Diffraction Data, Newtown Square, PA, USA.
29. S. Sasikumar and R. Vijayaraghavan, *Ceramics Internat.*, **34**, 1373 (2007).
30. R. Murungan, K.P. Rao and T.S.S. Kumar, *Bull. Mater. Sci.*, **26**, 523 (2003).
31. Vignoles, Ph.D. Thesis, University of Toulouse, France (1973).
32. I. Manjubala and M. Sivakumar, *Mater. Chem. Phys.*, **71**, 272 (2001).
33. Y.M. Park, S.C. Ryu, S.Y. Yoon, R. Stevens and H.C. Park, *Mater. Chem. Phys.*, **109**, 440 (2008).
34. S. Kanan, J.H.G. Ventura, A. Lemos and J.M.F. Ferreira, *Scr. Mater.*, **53**, 1259 (2005).

(*Received*: 16 August 2008; *Accepted*: 23 February 2009) AJC-7264